Supporting Information for Triazole-Stapled p53 Mimetics as MDM2 Inhibitors: Structural and Thermodynamic Origin of Enhanced Binding Affinity

Vikram Gaikwad[a,‡], Pushyaraga P. Venugopal[a,‡], and Rajarshi Chakrabarti[a*]

[a] *Department of Chemistry, Indian Institute of Technology Bombay, Mumbai 400076, India*

E-mail: rajarshi@chem.iitb.ac.in

1. Parameterization of triazole staple

The triazole staple segment, named as SEM, has been parameterized using the antechamber module of the AmberTools24, employing the General AMBER Force Field (GAFF) and AM1-BCC charge model. The initial 3D structure of the staple molecule was constructed using the Builder panel in Maestro.(Fig.S1) The symmetric staple ends were then capped using N-methyl (NME) and methyl acetate (ACE) to form a neutral segment. This structure was then input to Antechamber to assign GAFF atom types and calculate atomic partial charges using the semiempirical AM1-BCC method. This method provides a computationally efficient approximation of electrostatic potential-derived charges.

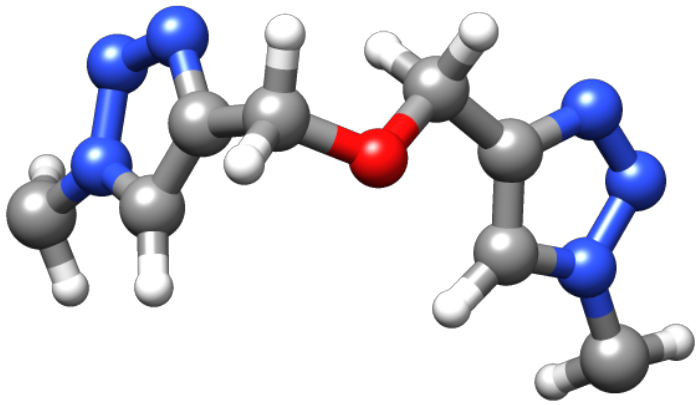

Fig. S1: Ball and Stick representation of the triazole crosslinker (SEM)

The *prepgen* module was used to generate a residue template for the staple segment. This file contains the information about atomic coordinates, atom types, charges, and connectivity suitable for the *LEaP* module. Complete parameters for the staple were generated using the *prepgen* module, with additional parameters added manually to describe the bonding between the staple and the side chains of p53. Missing bonded interactions not covered by *GAFF* were identified using the *parmchk2* tool and recorded in *frcmod* file. These included torsional parameters involving the linker atoms and adjacent peptide residues. The p53 peptide sequence selected for stapling was ETFSDLWRLLPEN (PDB ID: 1YCR), a region known to adopt an α-helical conformation upon binding. To enhance helicity and proteolytic stability while maintaining MDM2 affinity, we introduced the triazole staple between i and i+7 positions of the helix. Staple positions 4-11, 6-13, and 1-8 were selected based on the literature. The initial structure of each complex was prepared using PyMOL, utilizing the crystal structure of the MDM2-p53 complex as the template (PDB ID: 1YCR). The geometry of the staple was optimized to avoid the bad contacts within p53. Prior to parameterization,

the Cβ atom of residue 1/4/6 is connected to the Cβ atom of residue 8/11/the 13 by the triazole crosslinker (SEM) using bond command in *LEaP*. The *prepin, frcmod, and mol2* files were loaded into *LEaP* to build the full stapled peptide topology. The peptide topology is built using the Amberff19SB force field. The final structure was energy-minimized to verify stability before proceeding to molecular dynamics simulations.

2. System Details

Table ST1: System details include box dimensions, number of water molecules and number of ions in the box for respective p53-MDM2 complexes and free p53 peptides

System	**Box Dimensions** (nm×nm×nm)	**Number of water molecules**	**Number of Ions**
$p53^{wt}$-MDM2	6.33×6.33×6.33	23370	3 Cl^-
$p53^{4-11}$-MDM2	6.31×6.31×6.31	23346	3 Cl^-
$p53^{1-8}$-MDM2	6.30×6.30×6.30	23352	3 Cl^-
$p53^{6-13}$-MDM2	6.30×6.30×6.30	23334	3 Cl^-
$p53^{wt}$	4.72×4.72×4.27	3382	3 K^+
$p53^{4-11}$	4.71×4.71×4.71	3377	2 K^+
$p53^{1-8}$	4.75×4.75×4.75	3469	2 K^+
$p53^{6-13}$	4.73×4.73×4.73	3403	2 K^+

3. Convergence of RMSD Over Multiple Simulations

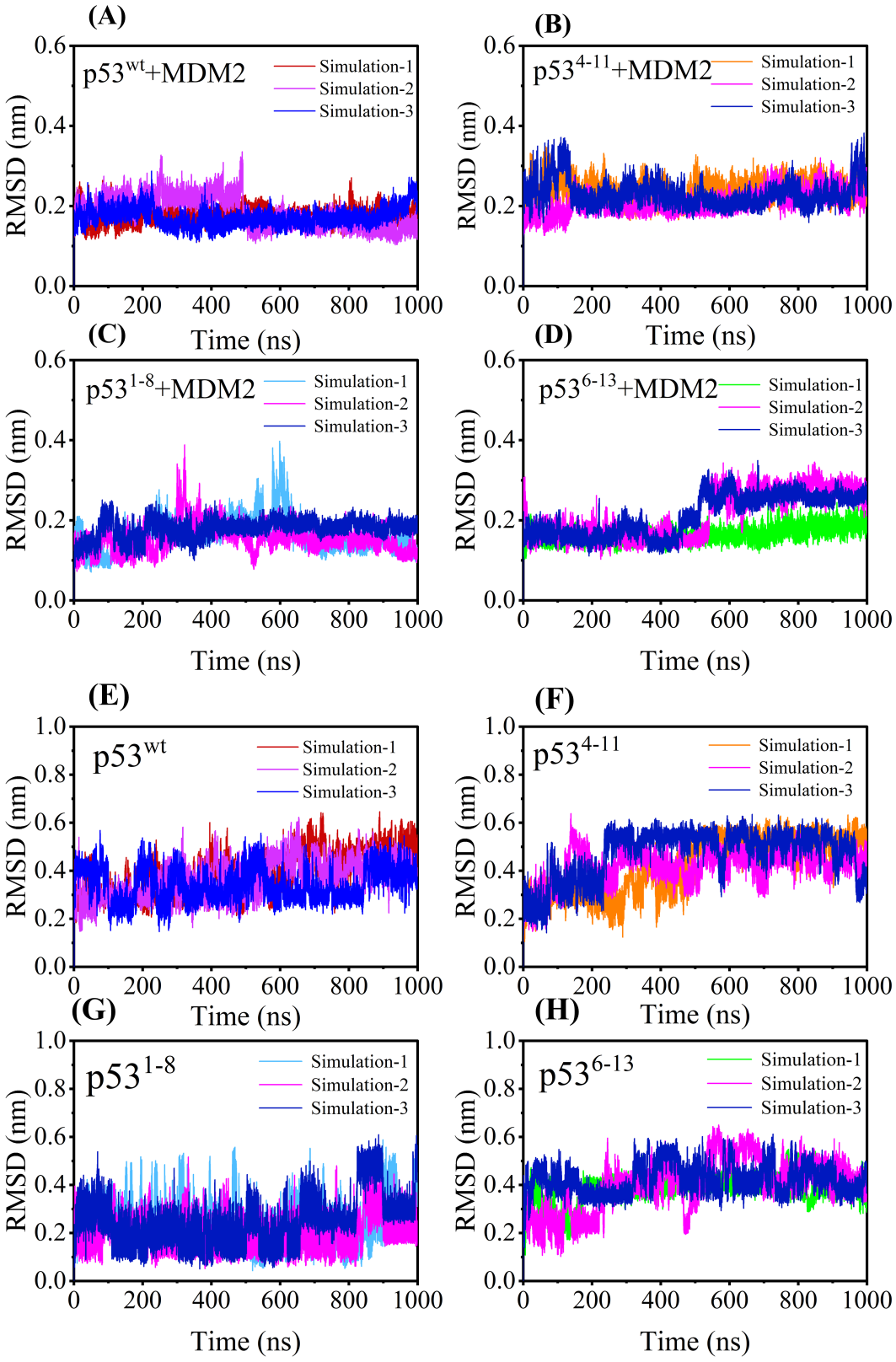

Fig. S2: Convergence of RMSD over three simulations: (A)$p53^{wt}$ + MDM2 ,(B)$p53^{4-11}$ + MDM2,(C)$p53^{1-8}$ + MDM2, (D)$p53^{6-13}$ + MDM2, (E)$p53^{wt}$,(F)$p53^{4-11}$, (G)$p53^{1-8}$, (H)$p53^{6-13}$

4. Convergence of ΔG_{bind} Over Multiple Simulations

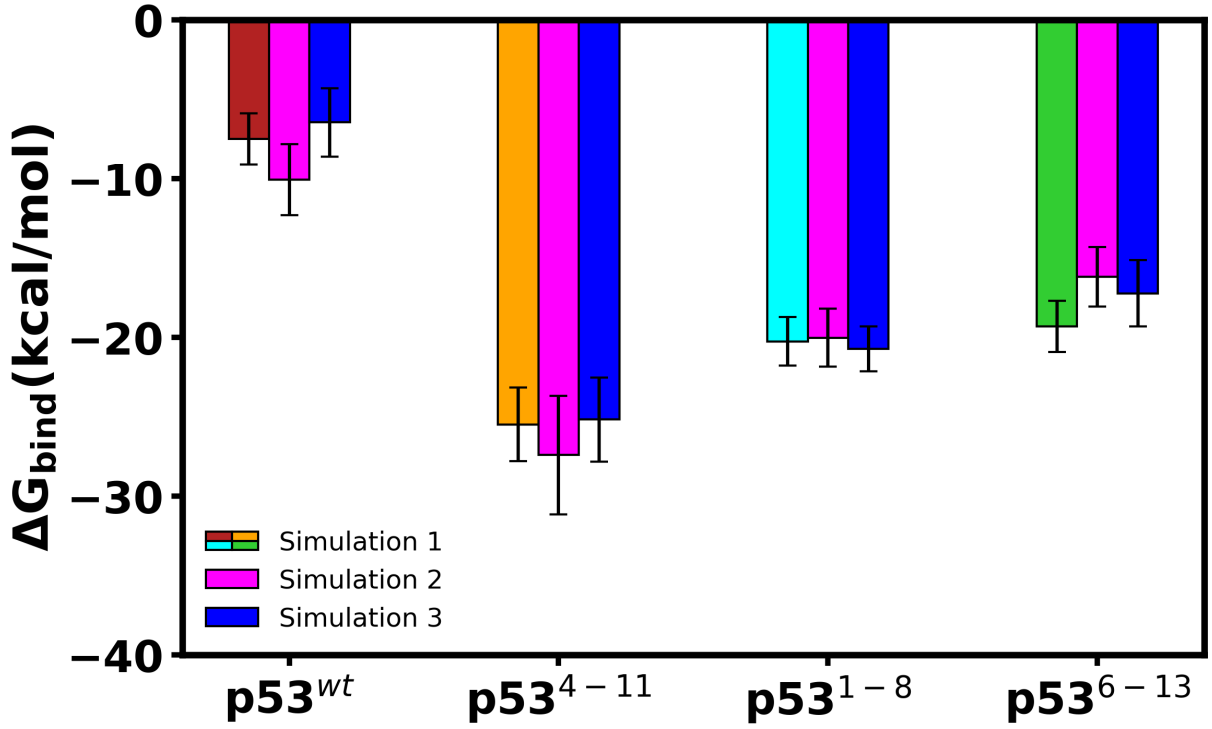

Fig. S3: Convergence of ΔG_{bind} over three simulations and they all are well converged. Simulation 1 follows the same colour scheme as the manuscript.

5. Free Energy Contribution of MDM2 Residues

Table ST2: Free energy contribution of MDM2 residues.

Residues of MDM2	Per-residue contribution to the ΔG_{bind} (kcal/mol)			
	$p53^{wt}$	$p53^{4-11}$	$p53^{1-8}$	$p53^{6-13}$
GLU2	0.7805	0.1319	0.6114	0.2856
THR3	-0.0742	-0.0640	0.0001	-0.0425
LEU4	-0.0072	0.0033	-0.0056	0.0104
VAL5	-0.0102	-0.0126	-0.0126	-0.0076
THR26	-0.0656	-0.2359	-0.0813	-0.0610
MET27	-0.2721	-0.4791	-0.5482	-0.2669
LYS28	-1.8344	-1.4093	-1.2393	-0.4513
GLU29	0.0522	-0.5565	0.0818	0.0526
VAL30	-0.2541	-0.3084	-0.2409	-0.3040
LEU31	-3.0231	-2.6316	-2.9478	-2.6123
PHE32	-0.9070	-3.5088	-0.8770	-0.6604
TYR33	-0.0914	-0.1612	-0.0818	-0.0467
LEU34	-0.7426	-0.4436	-0.7653	-0.6044
GLY35	-0.8664	-0.8761	-1.0113	-0.8497
GLN36	-0.2542	-0.8214	-0.2587	-0.1939
ILE38	-1.7876	-1.7439	-1.6313	-1.4557
MET39	-1.3311	-3.2029	-1.4158	-1.2211
ARG42	-0.5819	-8.5169	-0.4206	-0.3115
LEU43	0.0040	-0.0594	-0.0720	-0.0680
TYR44	-0.8388	-2.5391	-0.9513	-0.7590
ASP45	0.4127	0.5234	0.2769	0.2977
GLU46	0.2661	0.8163	0.1490	-0.2231
LYS47	-0.4271	-0.3857	-0.2517	-0.3086
GLN48	-0.1342	-0.0688	-0.0863	-0.1484
GLN49	-0.4224	-0.7110	-0.0046	-0.9654
HIE50	-0.8339	-0.7045	-1.2111	-2.2631

ILE51	-0.0017	0.0048	-0.0464	-0.2105
VAL52	-0.6091	-0.6870	-0.4585	-0.7232
LEU59	-0.0901	-0.0792	-0.0736	-0.1178
PHE63	0.0481	0.0822	0.0592	-0.1069
PHE68	-0.1322	-0.1904	-0.1683	-0.4198
SER69	-0.1613	-0.2335	-0.2215	-0.3186
VAL70	-1.3043	-1.9685	-1.3570	-3.4474
LYS71	-0.3483	-0.2105	-0.7291	-3.9824
GLU72	-0.0389	0.0071	-0.1694	-0.3431
HIE73	-0.7596	-0.2994	-1.3305	-2.1236
ARG74	-0.4440	-0.1734	-0.5182	-0.4811
LYS75	-0.1482	-0.1223	-0.1885	-0.1645
ILE76	-1.2984	-0.8091	-1.0874	-1.7480
TYR77	0.2957	-0.1576	-1.1468	0.3903
THR78	0.0050	0.0112	-0.0106	0.0668
ILE80	-0.0334	-0.0332	-0.1419	-0.1965
TYR81	-0.0290	-0.0001	-0.0094	-0.0012
Total	**-18.19**	**-32.82**	**-20.59**	**-27.11**

6. Convergence of Number of H-Bond Over Multiple Simulations

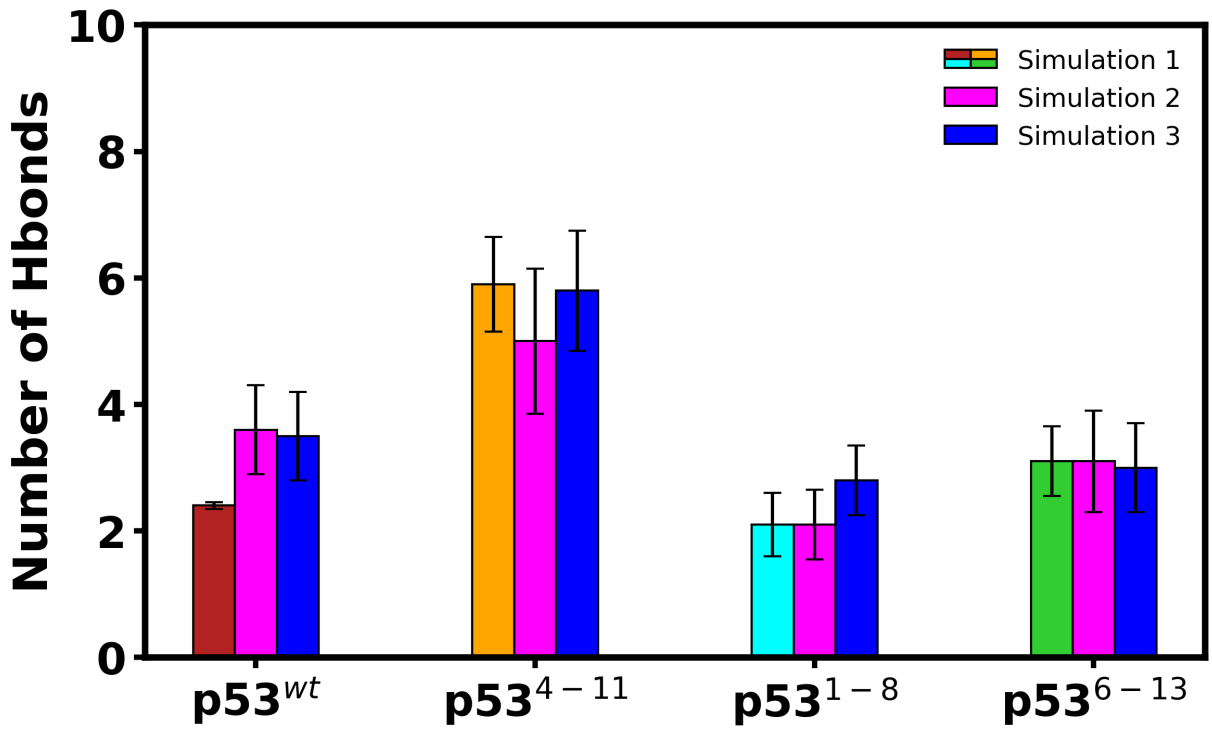

Fig. S4: Convergence of of H-Bond between p53 and MDM2 over three simulations and they all are well converged. Simulation 1 follows the same colour scheme as the manuscript.

7. H-Bond Pairs Present Between p53 and MDM2

Table ST3: H-bond pairs in each p53–MDM2 complex with their occupancies. Parentheses indicate the atom types involved in H-bonding. Residue pairs given in bold are present in all the systems

System	Residue-Pair (Donor --- Acceptor)	Occupancy (%)
$p53^{wt}$	**PHE3 (H) --- GLN49 (OE1)**	80.1
	TRP7 (HE1) --- LEU31 (O)	77.6
	TYR77 (HH) --- PRO11 (O)	19.3
	LYS28 (HZ1) --- GLU12 (OE1)	11.5
	LYS28 (HZ1) --- GLU12 (OE2)	11.5
$p53^{4-11}$	**TRP7 (HE1) --- LEU31 (O)**	85.0
	PHE3 (H) --- GLN49 (OE1)	55.7
	ARG42 (H21) --- GLU1 (OE1)	31.5
	ARG42 (H21) --- GLU1 (OE2)	30.5
	TYR44 (HH) --- GLU1 (OE2)	23.5
	ARG42 (HE) --- GLU1 (OE2)	22.4
	GLN49 (E21) --- GLU1 (OE1)	21.0
	TYR44 (HH) --- GLU1 (OE1)	19.4
	ARG42 (HE) --- GLU1 (OE1)	17.7
	GLN36 (E21) --- SEM(N3)	17.1
	GLN49 (E21) --- GLU1 (OE2)	16.4
	GLN49 (E21) --- GLU1 (O)	11.2
$p53^{1-8}$	**TRP7 (HE1) --- LEU31 (O)**	75.6
	PHE3 (H) --- GLN49 (OE1)	67.0
	GLN49 (E21) --- GLY1 (O)	12.6
$p53^{6-13}$	**TRP7 (HE1) --- LEU31 (O)**	95.2
	PHE3 (H) --- GLN49 (O)	76.6
	ARG74 (H11) --- GLY13 (O)	27.6
	LYS71 (HZ1) --- GLU1 (OE1)	23.7
	LYS71 (HZ1) --- GLU1 (OE2)	23.7
	TYR77 (HH) --- PRO11 (O)	12.9

8. Time evolution of dominant H-Bond Pairs Present Between p53 and MDM2

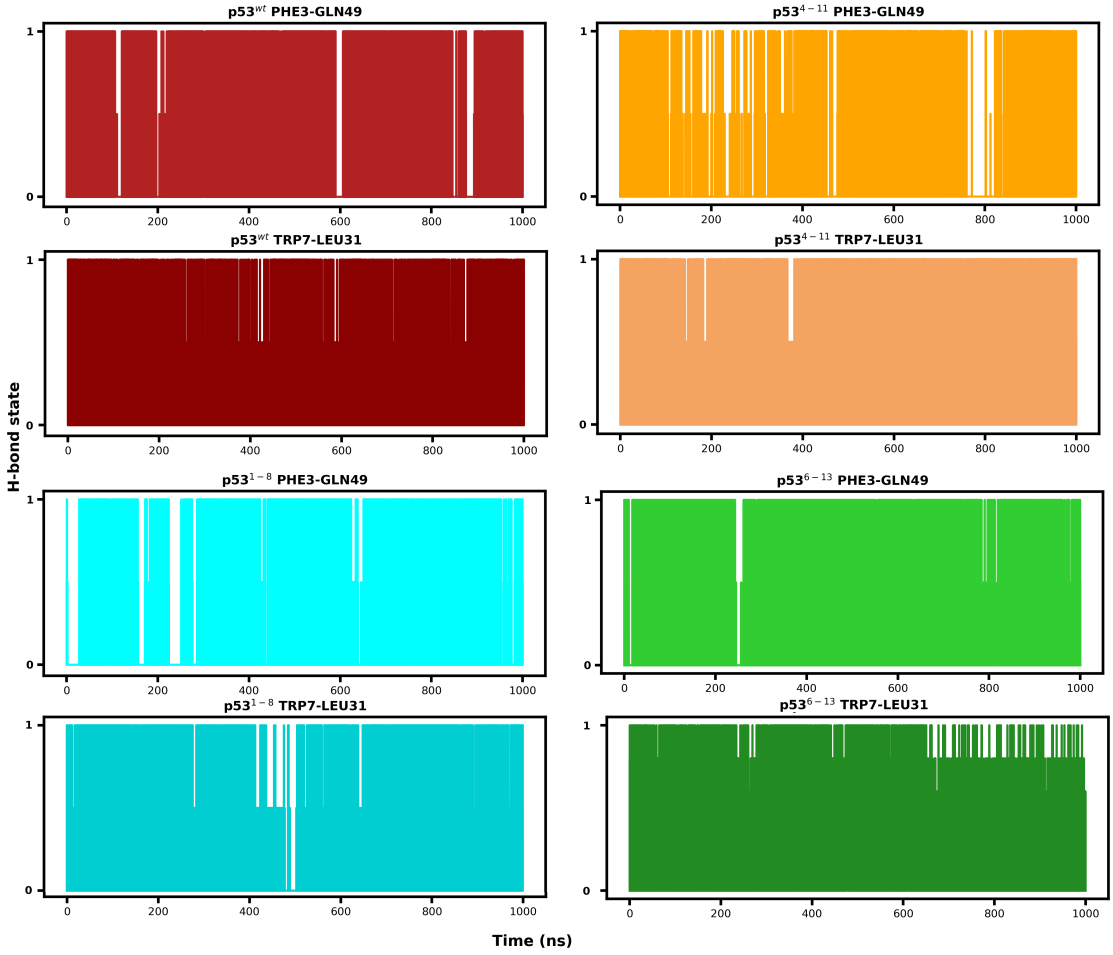

Fig. S5: Time series plot of two dominant H-Bond pairs between p53 and MDM2 over the complete trajectory. PHE3-GLN49 and TRP7-LEU31 are maintained throughout the trajectory.

9. Aromatic Interactions Between p53 and MDM2

Table ST4: Aromatic interactions between p53 and MDM2. Residue pairs given in bold (black) are present in all the systems. The residue pair in red font is present in only three systems.

System	Residue-Pair (MDM2-p53)	Occupancy (%)
$p53^{wt}$	**TYR44 – PHE3**	99.55
	PHE32 – TRP7 (5M)	87.65
	PHE68 – TRP7 (6M)	78.53
	PHE63 – TRP7 (6M)	5.96
	PHE32 – TRP7 (6M)	0.48
	PHE68 – PHE3	0.23
	TYR77 – TRP7 (6M)	0.03
$p53^{4-11}$	**TYR44 – PHE3**	99.44
	PHE68 – TRP7 (6M)	91.84
	PHE32 – TRP7 (5M)	77.87
	PHE32 – SEM (1T)	45.5
	PHE32 – SEM (2T)	38.41
	PHE63 – TRP7 (6M)	13.53
	PHE68 – PHE3	1.67
	TYR77 – TRP7 (6M)	0.82
	TYR77 – TRP7 (5M)	0.41
	PHE32 – TRP7 (6M)	0.18
	PHE68 – TRP7 (5M)	0.17
$p53^{1-8}$	**TYR44 – PHE3**	99.26
	PHE32 – TRP7 (5M)	84.69
	PHE68 – TRP7 (6M)	59.75
	PHE32 – TRP7 (6M)	3.13
	PHE63 – TRP7 (6M)	1.82
	PHE68 – PHE3	0.85
$p53^{6-13}$	**TYR44 – PHE3**	94.11
	PHE32 – TRP7 (5M)	91.18
	PHE68 – TRP7 (6M)	58.89
	TYR77 – SEM (1T)	51.73
	PHE63 – TRP7 (6M)	26.39
	PHE68 – PHE3	23.36
	PHE32 – TRP7 (6M)	6.49
	PHE68 – TRP7 (5M)	1.32
	PHE63 – PHE3	0.23
	PHE63 – TRP7 (5M)	0.13
	TYR81 – SEM (1T)	0.02

10. Ramachandran Maps

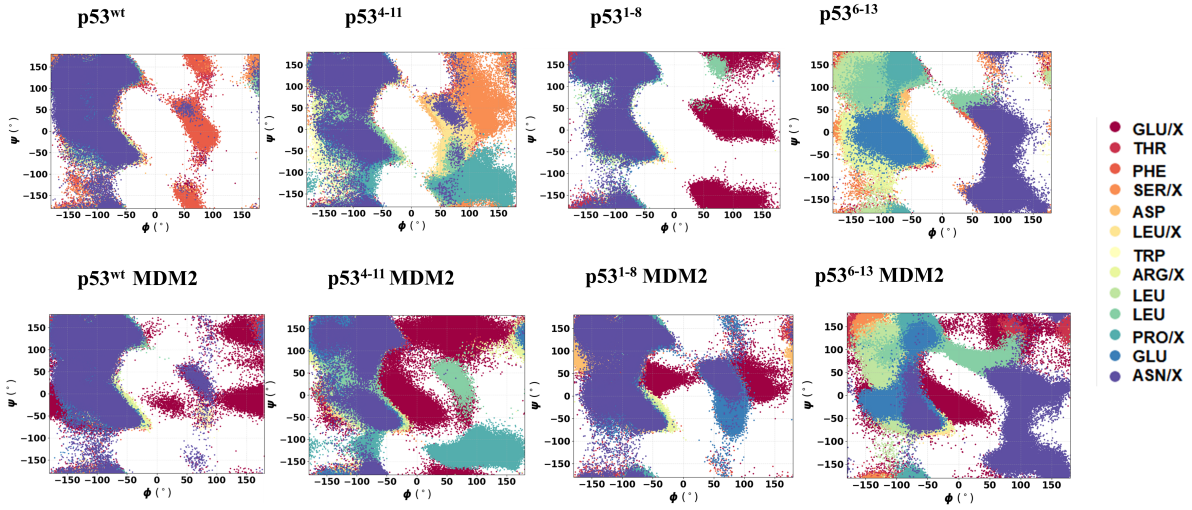

Fig. S6: Dihedral angle(ϕ/ψ) distribution of p53 peptides in the free and bound state

11. End-to-End to Distance

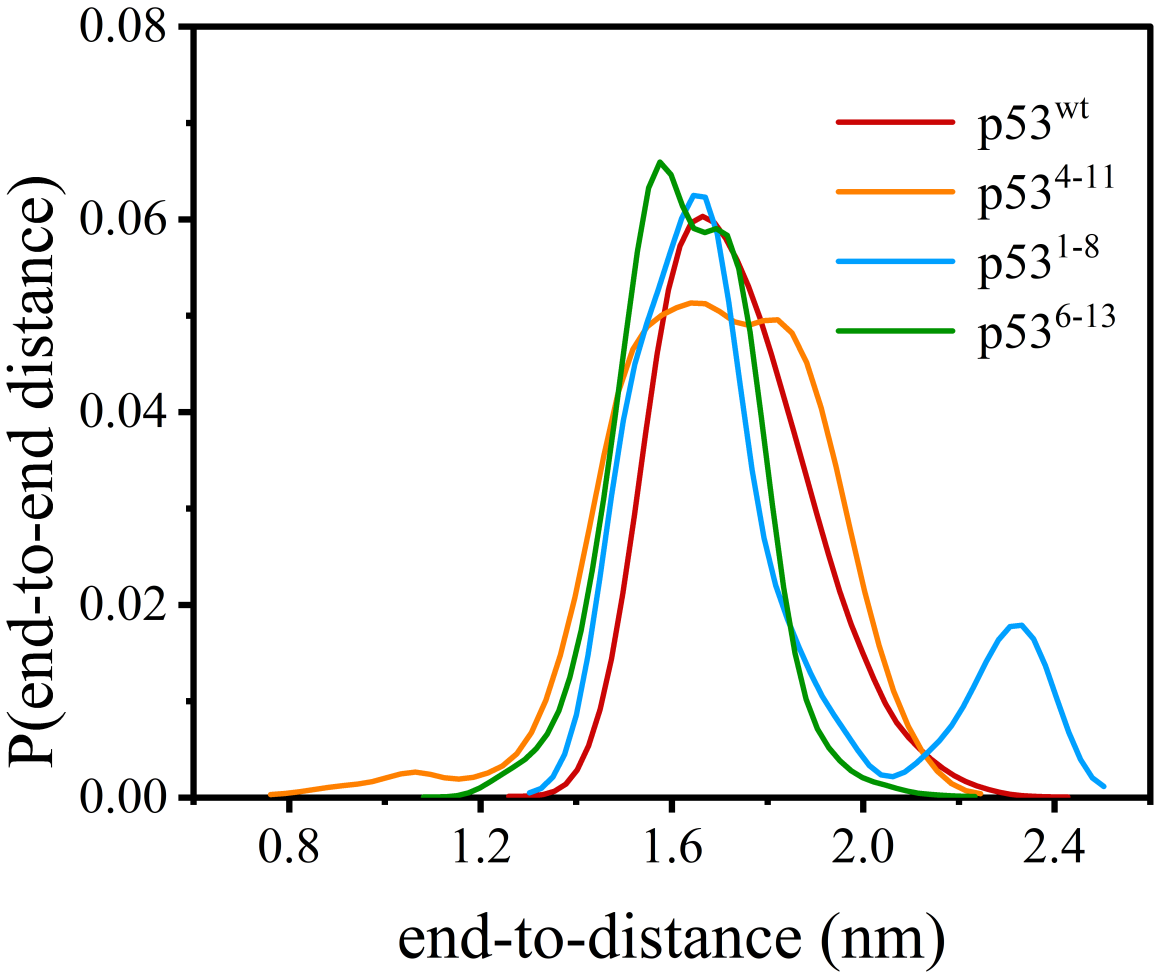

Fig. S7: Probability distribution of End-to-end distance between the Cα atoms of the terminal residues of p53 peptides in the bound state

12. Dictionary of Secondary Structure in Proteins (DSSP) of MDM2

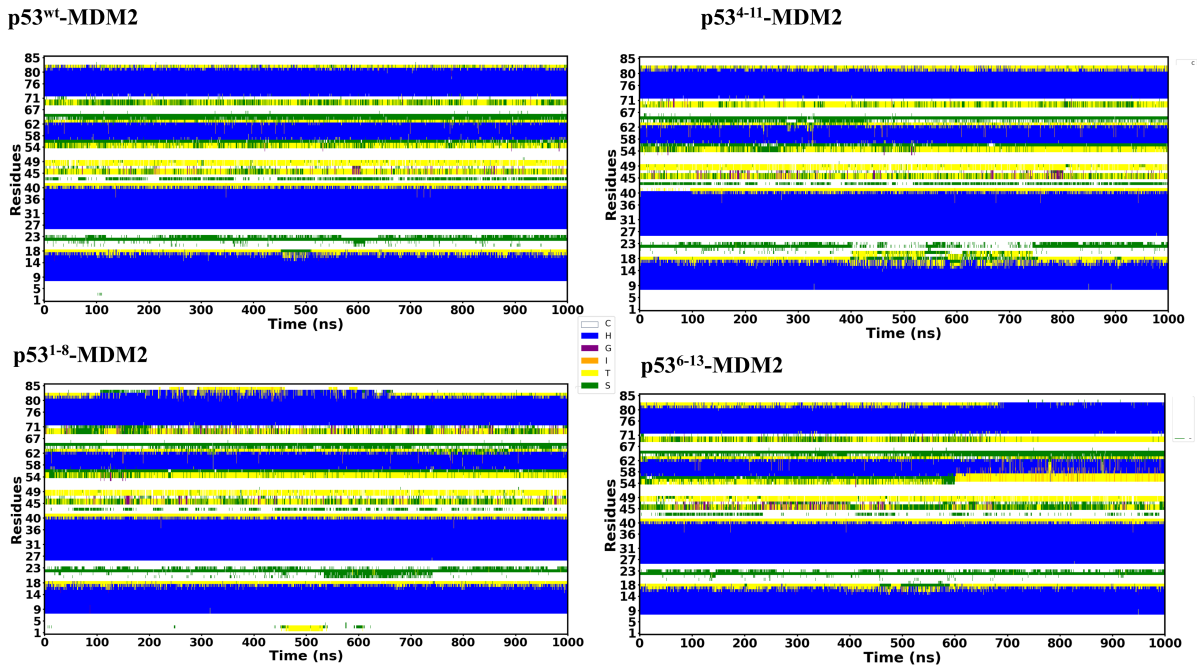

Fig. S8: DSSP of MDM2 bound state with p53, where respective colours indicate the type of secondary structure as C (Coil), H (α-Helix), G(3_{10}-helix), I (π-helix), T (Turn), S (Bend).

13. Residue-wise Conformational Entropy

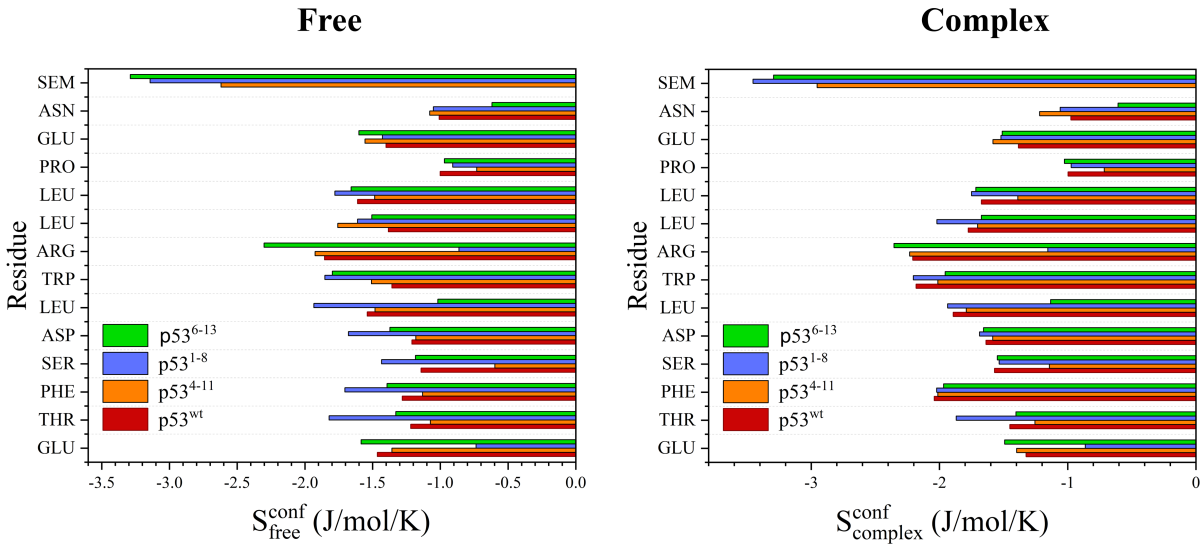

Fig. S9: Residue-wise conformational entropy of the p53-derived peptides in free and complex states.

14. RMSD based Clustring

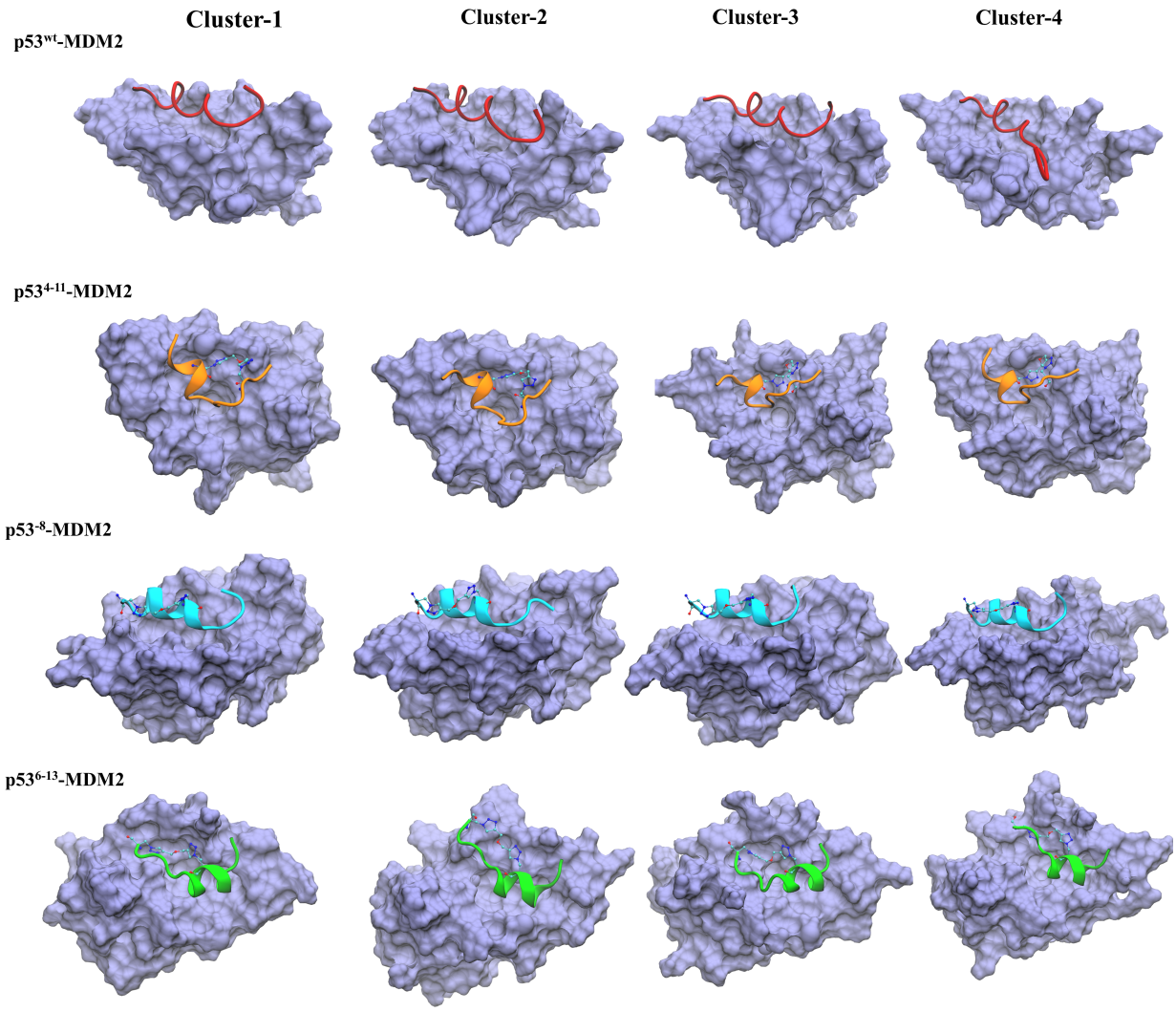

Fig. S10: The top four RMSD-based cluster central structures of the p53 peptides in the bound state are shown, showing that the binding mode varies depending on the position of the triazole staple.

15. Free Energy along fractional helicity

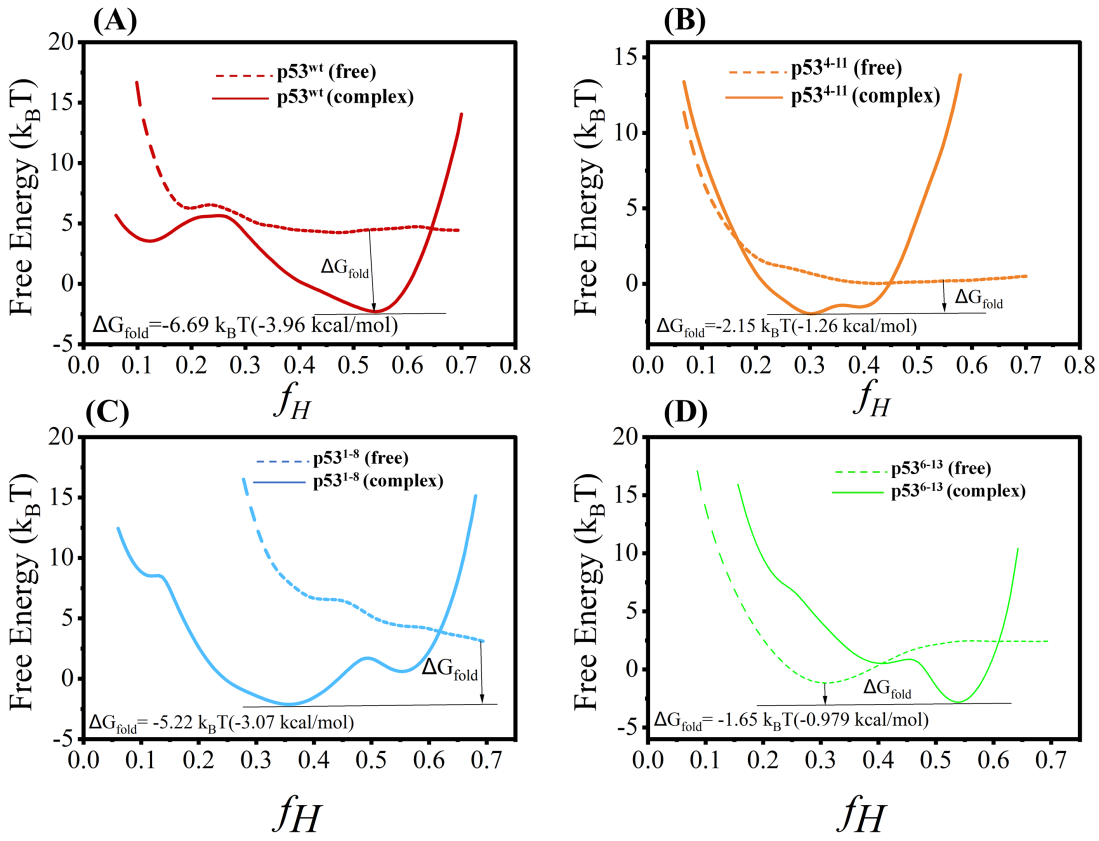

Fig. S11: Free energy plotted as a function of fractional helicity for both free (dotted) and complex (thick) states of p53-derived peptides.

16. Radial Distribution Function of water molecules around the peptide in the bound state

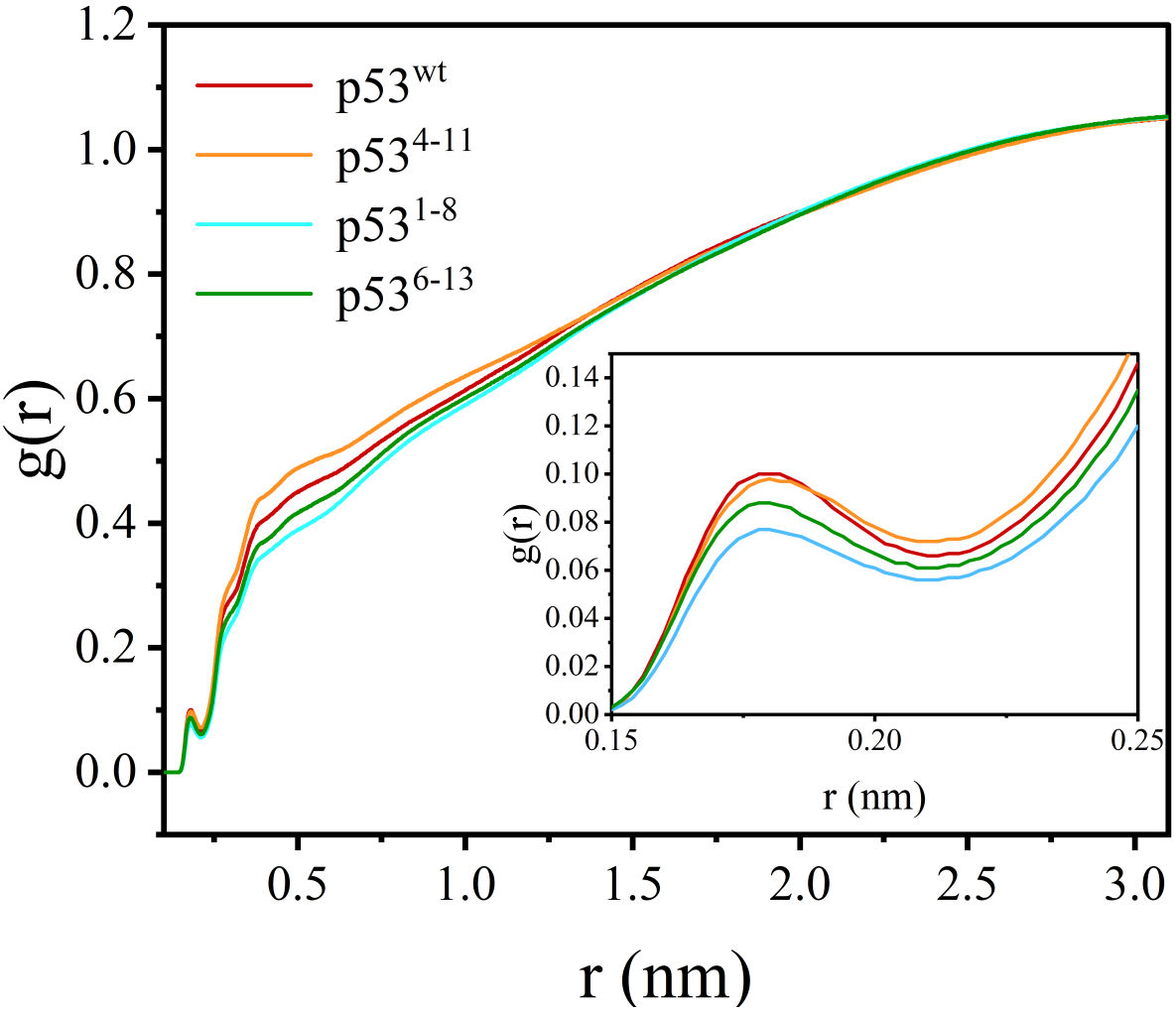

Fig. S12: Radial Distribution Function of water molecules around the p53 peptide in the bound state.

17. Number of Water Bridges

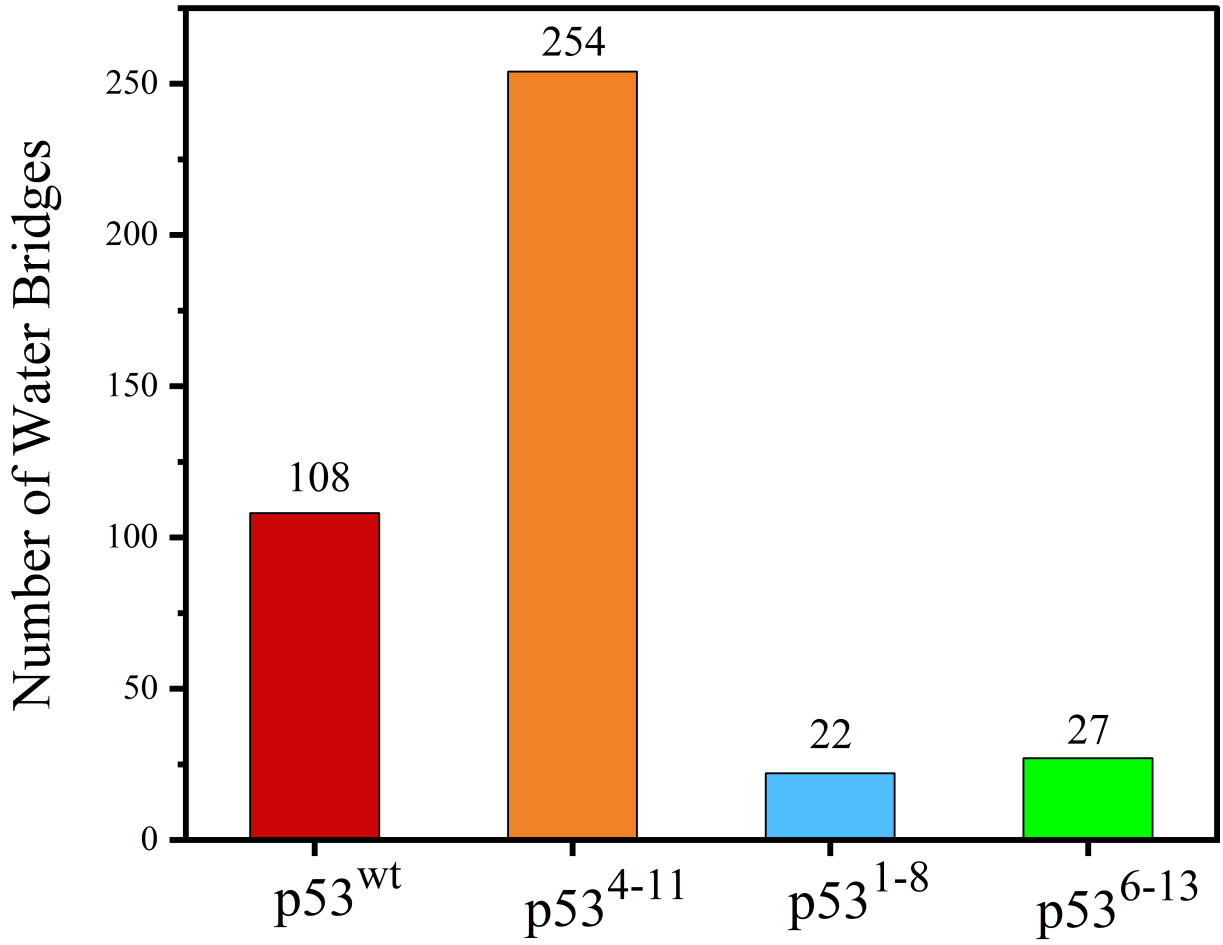

Fig. S13: Number of water bridges between p53 and MDM2 existing for more than 10% of the total simulation time.